

Eddy viscosity models in turbulent shear flows^(*)

H. I. ANDERSSON (TRONDHEIM)

INCORPORATION of algebraic eddy viscosity models in numerical schemes is considered, and problems arising from typical mixing length models are discussed. An explicit model for two-dimensional duct flow is derived, and the model is compared with existing models. The computed velocity profiles for fully developed flow correspond favourably with experimental results.

Rozważono uwzględnienie algebraicznych modeli lepkości wirowej w schematach obliczeniowych. Wyprowadzono jawną postać modelu dwuwymiarowego przepływu w kanale i przeprowadzono porównanie ze znanymi modelami zjawiska. Obliczone profile prędkości dla rozwiniętych przepływów wykazują dobrą zgodność z wynikami doświadczeń.

Рассмотрен учет алгебраических моделей вихревой вязкости в расчетных схемах. Выведен явный вид двумерной модели течения в канале и проведено сравнение с известными моделями явления. Вычисленные профили скорости для развернутых течений хорошо совпадают с результатами экспериментов.

Notations

- a parameter in Pai's velocity profile,
- A, A^+ parameter in van Driest's damping function,
- c constant in logarithmic velocity profile,
- f body force,
- h flow depth, channel half-width or pipe radius,
- h_0 upstream value of h ,
- l mixing length,
- m parameter in Pai's velocity profile,
- p pressure,
- $Re = u(h)h/\nu$,
- $Re_\tau = u_\tau h/\nu$,
- u, u' mean and fluctuating streamwise velocity,
- u_0 upstream value of $u(h)$,
- u_τ shear velocity,
- U freestream velocity or $u(h)$,
- v, v' mean and fluctuating cross-stream velocity,
- V velocity scale,
- x streamwise coordinate,
- y cross-stream coordinate.

Greek symbols

- α constant in turbulence model,
- β constant in turbulence model,

(*) Paper accepted for presentation at the XVII Biennial Fluid Dynamics Symposium in Sobieszewo in Poland, September 2-6, 1985.

- δ^* displacement thickness,
- ε eddy viscosity,
- $\varepsilon_i, \varepsilon_o$ inner and outer region eddy viscosities,
- κ von Kármán constant,
- λ dimensionless function in turbulence models,
- μ dynamic viscosity,
- ν kinematic viscosity,
- ρ density,
- τ, τ_w shear stress and wall shear stress.

1. Introduction

THE MOST common approaches to turbulence modelling are based on the classical eddy viscosity concept in which the turbulent shear stress is related to the rate of mean strain through an apparent turbulent viscosity. Even with the very simplest choice for this so-called eddy viscosity, i.e. a constant value throughout the flow field, interesting information may in some cases be extracted from numerical calculations, e.g. [7, 9].

In the present paper, however, turbulent shear flows will be considered, in which the cross-stream variation of the eddy viscosity cannot be neglected. In the first part of the paper, algebraic models for the eddy viscosity based on the mixing-length concept are considered. Some numerical results for a hydraulic-like thin shear-layer flow are presented, and numerical difficulties arising from the actual formulation of the eddy viscosity will be discussed.

In the second part of the paper, we consider a quite different approach devised by VAN DRIEST [17] for zero pressure gradient boundary layer flow. By assuming an explicit mixing-length model for the eddy viscosity, the velocity gradient can be obtained from the total shear stress distribution across the shear layer. Then it follows from the shear stress distribution that the eddy viscosity becomes an explicit function of the cross-stream coordinate only, and the resulting model does not depend explicitly on the cross-stream velocity gradient.

Following the basic arguments of VAN DRIEST [17], an explicit formula for the eddy viscosity can be derived, which exactly corresponds with the linear shear stress distribution in fully developed two-dimensional Poiseuille flow. Finally, the resulting formula will be compared with other algebraic models and data from the experimental investigation of HUSSAIN and REYNOLDS [10].

2. Reynolds stresses and eddy viscosity

We consider a two-dimensional steady flow with constant fluid properties. For boundary layers, or thin shear-layers, in which there exists a predominant direction of flow and with diffusion much larger in the cross-stream direction, the total shear stress in the Reynolds averaged streamwise momentum equation becomes

$$(2.1) \quad \tau = \mu \frac{\partial u}{\partial y} - \rho \overline{u'v'}.$$

Here the velocity fluctuations u' , v' denote the instantaneous deviations from the mean velocity components u , v . The bar represents the average of fluctuating quantities, and x , y are coordinates in the streamwise and cross-stream directions, respectively.

The *Reynolds stress tensor* $-\overline{\rho u'v'}$ represents the exchange of momentum between the turbulence and the mean flow. According to a classical approach suggested by Boussinesq, the unknown Reynolds stress is linearly related to the gradient of the mean flow, i.e.

$$(2.2) \quad -\overline{\rho u'v'} = \rho \varepsilon \frac{\partial u}{\partial y}.$$

Here ε is the turbulent exchange coefficient for momentum, which is called *turbulent* or *eddy viscosity*. By contrast with the molecular viscosity μ in Eq. (2.1), however, the eddy viscosity is not a fluid property but depends on the local flow conditions and the state of turbulence.

3. Thin shear-layer momentum equation

Utilizing the eddy viscosity hypothesis (2.2), the Reynolds averaged streamwise momentum equation is commonly written as

$$(3.1) \quad u \frac{\partial u}{\partial x} + v \frac{\partial u}{\partial y} = -\frac{1}{\rho} \frac{\partial p}{\partial x} + f + \nu \frac{\partial}{\partial y} \left[\left(1 + \frac{\varepsilon}{\nu} \right) \frac{\partial u}{\partial y} \right].$$

The constant kinematic viscosity μ/ρ has been denoted by ν , and f may represent an applied body force per unit mass of the fluid.

In order to solve the mean flow equation (3.1), the eddy viscosity must be known. The very simplest approximation of the turbulent effects on the mean flow can be achieved by assuming ε to be equal to the molecular viscosity multiplied by some constant factor, i.e.

$$(3.2) \quad \frac{\varepsilon}{\nu} = \text{constant},$$

the constant being typically of the order 10^2 . Nevertheless, by using this crude approximation, interesting information can in some cases be extracted from numerical calculations, as demonstrated recently by HANSON, SUMMERS and WILSON [7] and HIRT [9].

From the numerical point of view, the constant eddy-viscosity approach (3.2) does not require any modifications of computer codes designated for laminar flow calculations. The only implication of the turbulence is the increased effective diffusivity $(\nu + \varepsilon)$, which in general quenches instabilities arising from diffusion-like truncation errors, see e.g. HIRT [8].

For shear layers in the vicinity of solid walls, however, the cross-stream variation of the eddy-viscosity is significant, and a more appropriate model for ε should be selected. Either the eddy-viscosity is obtained from an algebraic model, or by solving some additional turbulence transport equations, the resulting spatial variation of the effective diffusivity in Eq. (3.1) may give rise to numerical difficulties. This will be exemplified in the following section by means of some simple models based on the mixing-length concept.

4. Mixing-length models

Numerous algebraic models for the eddy viscosity are based on the *mixing-length* hypothesis introduced by PRANDTL [13]. He described the variation of the eddy viscosity by postulating its proportionality to the local values of the turbulent length scale l and the mean value V of the fluctuating velocities. He furthermore assumed that V should be related to the local mean velocity gradient through this length scale, i.e.

$$(4.1) \quad \varepsilon = lV, \quad V = l|\partial u/\partial y|.$$

The turbulent length scale l , i.e. the mixing length, is usually of the same order as the cross-stream length scale of the mean flow. By adopting the mixing-length hypothesis (4.1), an empirical model for l , rather than for ε , must be selected.

4.1. Cebeci and Chang model

Among the most popular mixing-length formulations is the model derived by VAN DRIEST [17]. The resulting expression for the eddy viscosity becomes

$$(4.2) \quad \varepsilon = [1 - \exp(-y/A)]^2 l^2 \left| \frac{\partial u}{\partial y} \right|.$$

The term in the square brackets accounts for the damping effect of the thin viscous sublayer close to the wall, so that the mixing length $l = \kappa y$ outside the viscous shear layer is effectively modified near the wall. The damping constant A in Eq. (4.2) can be expressed as

$$(4.3) \quad A = A^+ \nu / u_\tau,$$

where

$$(4.4) \quad u_\tau = (\tau_w/\rho)^{1/2}$$

is the friction or *shear velocity*, τ_w is the wall friction, and the dimensionless constant $A^+ = 26$.

VAN DRIEST's analysis [17] was restricted to zero pressure gradient boundary layer flows, for which the linear relation $l = \kappa y$ is a reasonable assumption. In the numerical analyses of developing turbulent flows in ducts, however, CEBECI and CHANG [4] and CEBECI [3] used

$$(4.5) \quad l = h \left[0.14 - 0.08 \left(1 - \frac{y}{h} \right)^2 - 0.06 \left(1 - \frac{y}{h} \right)^4 \right]$$

in the fully developed flow region. This mixing-length formulation was obtained by NIKURADSE [11] for turbulent pipe flow, h being the radius of the pipe. If applied to a plane duct, however, h denotes the half width of the duct. It should be noticed that

$$(4.6) \quad \frac{l}{h} \cong \begin{cases} 0.40 \left(\frac{y}{h} \right) - 0.44 \left(\frac{y}{h} \right)^2, & y \ll h, \\ 0.14, & y = h \end{cases}$$

so that the linear relation $l = \kappa y$ is recovered from Eq. (4.5) near the wall, the von Kármán constant κ being equal to 0.40.

4.2. Modified Cebeci and Smith model

Near the entrance of a pipe, the shear layers develop in the region close to the wall, and the inviscid core region is slightly accelerated. In this entrance region, CEBECI and CHANG [4] used the well-known two-layer model:

$$(4.7) \quad \begin{aligned} \varepsilon_i &= [1 - \exp(-y/A)]^2 (\kappa y)^2 \left| \frac{\partial u}{\partial y} \right|, \\ \varepsilon_o &= \alpha \cdot \delta^* \cdot U \end{aligned}$$

due to CEBECI and SMITH [5]. They regarded the turbulent shear layer as a composite layer characterized by an inner and outer region, so that the inner region model ε_i should be matched with the outer region model ε_o by the requirement of continuity in ε . The constant outer region model (4.7)₂ is expressed in terms of the displacement thickness δ^* and the velocity U at the outer edge of the shear layer, and α is an empirical constant.

The inner region model (4.7)₁ exhibits the same form as Eq. (4.2). However, in order to avoid the explicit appearance of the velocity gradient, the latter can be derived from the well-established logarithmic velocity profile

$$(4.8) \quad \frac{u(y)}{u_\tau} = \frac{1}{\kappa} \ln \left(\frac{y u_\tau}{\nu} \right) + c.$$

Thus ANDERSSON [1] replaced the Cebeci and Smith model defined by Eqs. (4.7) with the modified set of model equations:

$$(4.9) \quad \begin{aligned} \varepsilon_i &= [1 - \exp(-y/A)]^2 \kappa y u_\tau, \\ \varepsilon_o &= \beta h u_\tau. \end{aligned}$$

In accordance with the first part of Prandtl's mixing-length hypothesis, Eq. (4.1), the outer region model (4.9)₂ exhibits proportionality to a velocity scale and a length scale. However, instead of relating the velocity scale to the gradient of the mean flow, we simply take $V = 0.5u_\tau$, while the length scale l is set equal to $0.14 h$, i.e. the value of the mixing-length (4.5) on the symmetry line. Thus the dimensionless constant β becomes equal to 0.07. Taking into account the fact that the damping factor in Eq. (4.9)₁ vanishes for $y u_\tau / \nu \gg A^+$, the position at which ε_i becomes equal to ε_o is readily found as $y \cong h \beta / \kappa = 0.175h$.

4.3. Numerical results for hydraulic-like thin shear-layer flow

In a recent numerical investigation of the decelerating supercritical hydraulic flow along an inclined bed, ANDERSSON [1] employed the Cebeci and Chang model as well as the modified Cebeci and Smith model for the eddy viscosity. The numerical solutions were obtained using a parabolic finite-difference scheme, starting the calculations at $x = 0$ by specifying the two-parameter profile

$$(4.10) \quad \frac{u(y)}{u(h)} = 1 - a \left(1 - \frac{y}{h} \right)^2 - (1 - a) \left(1 - \frac{y}{h} \right)^{2m}$$

derived by PAI [12]. Comparing with experimental data for fully developed plane channel flow, Pai estimated that $m = 16$ and $a = 0.33$. In order to simulate a rather undeveloped upstream velocity profile, however, a was taken as 0.05 in Refs. [1, 2].

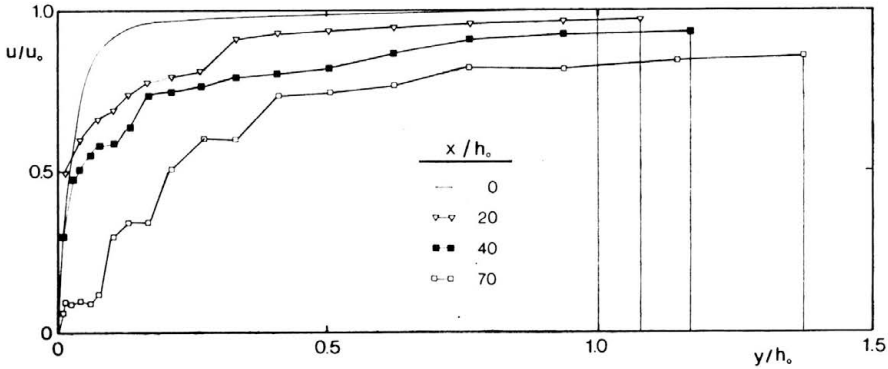


FIG. 1. Velocity profiles for supercritical hydraulic flow, $Re_\tau = 1005$. Cebeci and Chang model.

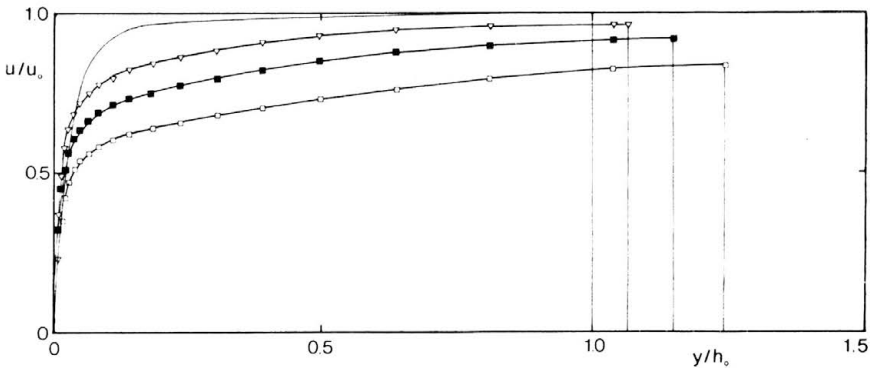


FIG. 2. Velocity profiles for supercritical hydraulic flow, $Re_\tau = 1005$. Modified Cebeci and Smith model. The symbols are defined in Fig. 1.

Predicted cross-stream velocity profiles are displayed in Fig. 1 and 2 for a flow with the Reynolds number $Re \equiv u(h)h/\nu$ based on the surface velocity $u(h)$ being equal to $3.31 \cdot 10^4$ at the upstream end of the incline. The corresponding Reynolds number based on the shear velocity can be derived from Eq. (4.10) as

$$(4.11) \quad Re_\tau \equiv \frac{u_\tau h}{\nu} = \sqrt{2[a+m(1-a)]} Re,$$

which becomes $Re_\tau = 1005$ for the actual choice of parameters.

By using the Cebeci and Chang mixing-length model, Eqs. (4.2) and (4.5), the erratic velocity profiles in Fig. 1 were obtained. These profiles clearly demonstrate the problems which may arise as a turbulence model is introduced in a numerical scheme. In the present case the remedy was to replace the Cebeci and Chang model with the modified Cebeci and Smith model defined by Eqs. (4.9). For the same set of parameters as in Fig. 1, smooth profiles were obtained at the various streamwise positions, some of which are shown in Fig. 2.

This dramatic improvement in the results is related to the particular form of the models considered. More specifically, the product of the increasing function l^2 and the strongly decreasing velocity gradient $\partial u/\partial y$ in Eq. (4.2) may result in a more or less pronounced

peak in the eddy viscosity profile. For instance, the eddy viscosity distribution derived from the Cebeci and Chang model exhibits a pronounced peak close to the wall, as shown in Fig. 3. The velocity profiles in Fig. 1 thus demonstrate how the irregularities caused by this peak are diffused over the cross-section as the solution is marched in the downstream direction.

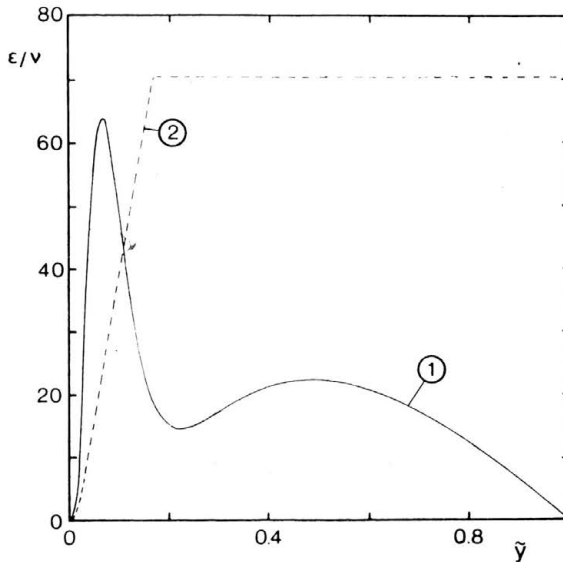


FIG. 3. Eddy viscosity profiles, $Re_\tau = 1005$. 1 — Cebeci and Chang model, Eqs. (4.2) and (4.5); 2 — modified Cebeci and Smith model, Eq. (4.9).

In present section we have shown the sometimes crucial effect of the explicit dependence on the velocity gradient which is exhibited by most mixing-length models. By a simple reformulation of the turbulence model, this problem was easily eliminated.

5. Eddy viscosity models

In the famous paper by VAN DRIEST [17] an explicit formula for the eddy viscosity distribution across a turbulent boundary layer was derived. By assuming the total shear stress to be constant near the wall, the sometimes problematic velocity gradient could be eliminated, and an algebraic relation for ε as function of the distance from the wall, y , could be derived. The underlying assumption in van Driest's analysis, i.e. the total shear stress being a constant, is a reasonable approximation in the inner part of a zero pressure gradient boundary layer flow. In the present section, however, van Driest's analysis is carried over to confined flows in which the total shear decreases from the wall towards the center of the duct.

5.1. Present formulation for duct flow

For fully developed two-dimensional duct flow, the total shear stress is a linearly decreasing function, according to the dimensionless relation

$$(5.1) \quad \left(1 + \frac{\varepsilon}{\nu}\right) \frac{\partial \tilde{u}}{\partial \tilde{y}} = (1 - \tilde{y}) \text{Re}_\tau$$

which can be derived as the integrated form of the momentum equation (3.1). In Eq. (5.1), however, we have introduced the dimensionless variables

$$(5.2) \quad \tilde{u} = u/u_\tau, \quad \tilde{y} = y/h.$$

It should be noted that Eq. (5.1) applies for pressure-driven flow in a plane channel, i.e. Poiseuille flow, as well as for pipe flow. In both cases h denotes the distance from the symmetry line to the walls.

Now, a proper model for ε must be selected, and the Cebeci and Chang model is adopted in the present investigation. CEBECI [3] and CEBECI and CHANG [4] used the model equations (4.2) and (4.5) for the entire shear layer in the fully developed region of a turbulent pipe flow. However, while Cebeci and Chang incorporated the eddy viscosity model in their numerical scheme, we solve Eq. (5.1) directly for the velocity gradient, i.e.

$$(5.3) \quad \frac{\partial \tilde{u}}{\partial \tilde{y}} = \frac{2(1 - \tilde{y}) \text{Re}_\tau}{1 + \sqrt{1 + 4\lambda}}$$

where λ is a dimensionless function of the distance from the wall and of the mixing length. Here λ can be expressed in terms of the dimensionless coordinate \tilde{y} or, alternatively, in terms of the inner variable $y^+ \equiv yu_\tau/\nu = \tilde{y}\text{Re}_\tau$, i.e.

$$(5.4) \quad \lambda = [1 - \exp(-\tilde{y}\text{Re}_\tau/A^+)]^2 \tilde{l}^2 \text{Re}_\tau^2 (1 - y) = [1 - \exp(-y^+/A^+)]^2 l^{+2} \cdot (1 - y^+ \text{Re}_\tau^{-1}),$$

where $\tilde{l} \equiv l/h$ and $l^+ \equiv lu_\tau/\nu = \tilde{l}\text{Re}_\tau$. With the velocity gradient across the shear layer given analytically by Eq. (5.3), the shear stress distribution (5.1) can be solved for the eddy viscosity to give

$$(5.5) \quad \frac{\varepsilon}{\nu} = \frac{1}{2} [\sqrt{1 + 4\lambda} - 1].$$

Thus the eddy viscosity becomes an explicit function of the cross-stream coordinate, the Reynolds number being a parameter in the model.

It should be noted that Eq. (5.5) can be approximated as

$$(5.6) \quad \frac{\varepsilon}{\nu} \approx \begin{cases} \lambda & \text{for } \lambda \ll 1, \\ \sqrt{\lambda} & \text{for } \lambda \gg 1 \end{cases}$$

for small and large values of λ , respectively. The latter approximation which applies away from the walls can be rewritten as

$$(5.7) \quad \frac{\varepsilon}{u_\tau h} = \frac{\varepsilon/\nu}{\text{Re}_\tau} \approx \tilde{l}(1 - \tilde{y})^{\frac{1}{2}}.$$

This rescaling reveals that the dimensionless eddy viscosity becomes an explicit function of \tilde{y} over the main part of the shear layer.

5.2. Models of Reichardt and van Driest

VAN DRIEST [17] derived an explicit formula for the eddy viscosity in a turbulent boundary layer by assuming the total shear stress to be constant near the wall. The resulting formula takes the same form as Eq. (5.5), the dimensionless function λ being

$$(5.8) \quad \lambda = [1 - \exp(-y^+/A^+)]^2 (\kappa y^+)^2$$

because the linear relation $l^+ = \kappa y^+$ was employed for the mixing length distribution.

A common feature of van Driest's formula and the present model is that both are derived analytically from the momentum equation by using an algebraic model for the mixing-length. REICHARDT [14], on the other hand, showed that experimental data can be fitted by the expression

$$(5.9) \quad \frac{\varepsilon}{u_\tau h} = \frac{\kappa}{6} (3 - 4\tilde{y} + 2\tilde{y}^2)(2\tilde{y} - \tilde{y}^2).$$

This formula closely approximates the observed variation of ε across the duct, except in the vicinity of the walls.

According to HUSSAIN and REYNOLDS [10], the empirical formula (5.9) due to Reichardt was extended by CESS [6] to include the near-wall region. The Cess expression for duct flow cited in [10], however, obviously suffers from misprints. This is easily seen by the fact that ε vanishes at $y = \sqrt{7} - 2 \approx 0.646$. Accordingly, we resort to the calculated curves presented in [10] for comparative use in the present paper.

5.3. Comparisons and discussions

First of all we reconsidered the two models compared in Fig. 3. Eddy viscosity curves for $Re_\tau = 520$ are displayed in Fig. 4. This particular Reynolds number corresponds

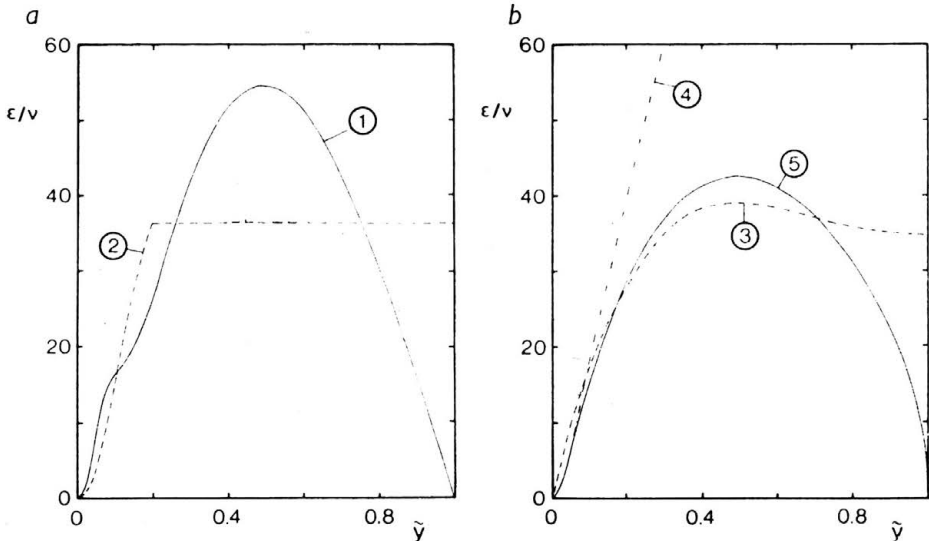


FIG. 4. Various eddy viscosity curves obtained for $Re_\tau = 520$. a) 1 — Cebeci and Chang model, Eqs. (4.2) and (4.5), 2 — modified Cebeci and Smith model, Eq. (4.9); b) 3 — REICHARDT [14], Eq. (5.9), 4 — VAN DRIEST [17], Eqs. (5.5) and (5.8), 5 — present formula, Eqs. (5.5) and (5.4).

to the case for which PAI [12] estimated the parameters m and a in the velocity profile (4.10) to be 16 and 0.33, respectively. Figure 4a demonstrates that the extreme behaviour of the Cebeci–Chang model exhibited in Fig. 3 has disappeared, and only a modest bulging of the profile remains in the near wall region. Figure 4b shows that the present formula is fairly close to the curve-fit polynomial (5.9) due to REICHARDT [14]. At the centerline, however, any model based on the mixing length hypothesis (4.1) due to PRANDTL [13], has to give $\varepsilon = 0$ because of the vanishing velocity gradient at the symmetry line.

The model derived by VAN DRIEST [17] is observed to approach the present model as y tends to zero, while very large turbulent viscosities are predicted away from the wall region. In their numerical investigations of duct flows, TAYLOR *et al.* [15, 16] used the van Driest formula in the near wall region, i.e. for $0 < \tilde{y} < 0.158$, and took the eddy viscosity to be constant over the remaining part of the cross-section. To employ the van Driest model in the near wall region is obviously a quite good approximation, even for confined flows. However, to represent the eddy viscosity by a constant value throughout the region $0.158 < \tilde{y} < 1.0$ seems to be a rough approximation, the value of ε/ν at $\tilde{y} = 0.158$ being slightly below 30.

The present eddy viscosity model is also compared with results from the comprehensive experimental investigation by HUSSAIN and REYNOLDS [10]. They obtained the eddy viscosity profiles shown in Figs. 5 and 6 from Eq. (5.1) by using experimental data for the mean

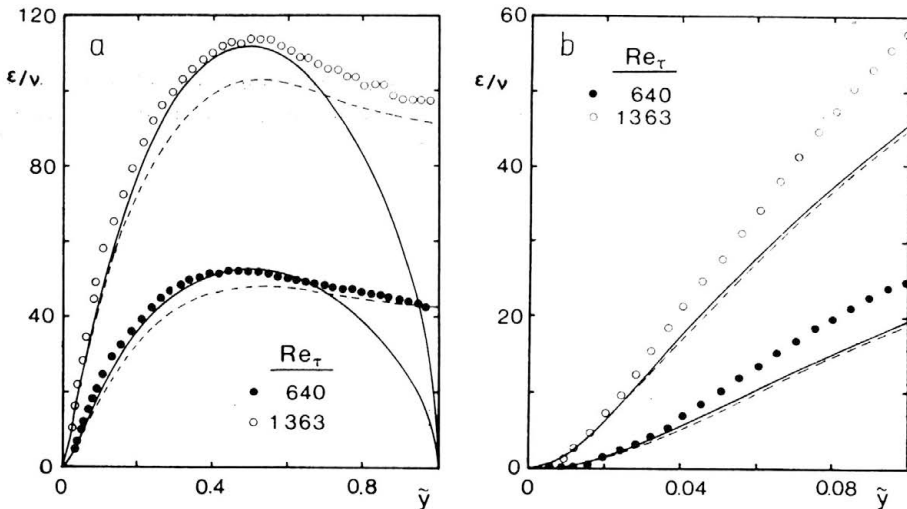


FIG. 5. Eddy viscosity profiles compared with experimental data (symbols) of HUSSAIN and REYNOLDS [10]. a) cross-section, b) wall region. Broken line denotes Cess-formula cited in [10]. Solid line denotes present model, Eqs. (5.4) and (5.5).

velocity profiles. The curves corresponding to the Cess formula are taken from Ref. [10]. It is observed from Fig. 5b that both formulations deviate from the experimental data in the near wall region. However, for $\tilde{y} < 0.7$ the present model compares more favourably to the experimental results than does the Cess formula.

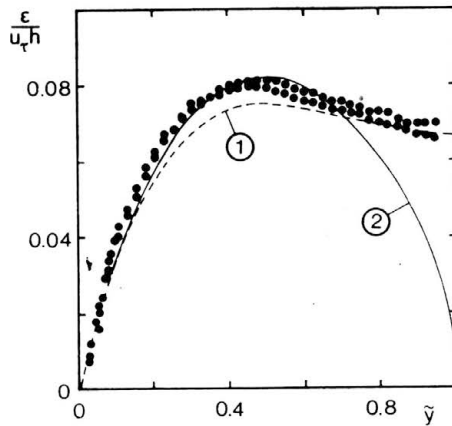


FIG. 6. Eddy viscosity profiles compared with experimental data (symbols) of HUSSAIN and REYNOLDS [10] for $Re_\tau = 640, 1013$ and 1363 . 1 — REICHARDT [14], Eq. (5.9), 2 — present approximate formula, Eq. (5.7).

By rescaling the data in Fig. 5, Hussain and Reynolds obtained an eddy viscosity distribution which is apparently independent of the Reynolds number away from the wall, as shown in Fig. 6. This Reynolds number independence is consistent with the present approximate model (5.7), as well as the curve-fit (5.9) due to REICHARDT [14]. While the outer part of the modified Cebeci and Smith model (4.9)₂ gives $\epsilon/u_\tau h = \beta = 0.07$, the maximum value obtained from Eq. (5.7) is slightly above 0.08 and fairly close to the experimental data in Fig. 6.

Finally, in order to see if the present eddy viscosity formulation is consistent with a proper velocity profile, Eq. (5.3) was integrated numerically from the wall to the centerline. Figure 7 shows that the resulting velocity profile for $Re_\tau = 640$ is close to $\tilde{u} = y^+$ near the wall, and approximates the logarithmic law (4.8) for $y^+ \gtrsim 30$. Near the centerline, a slight wake-like form is exhibited. Furthermore, the predicted profiles shown in Fig. 8

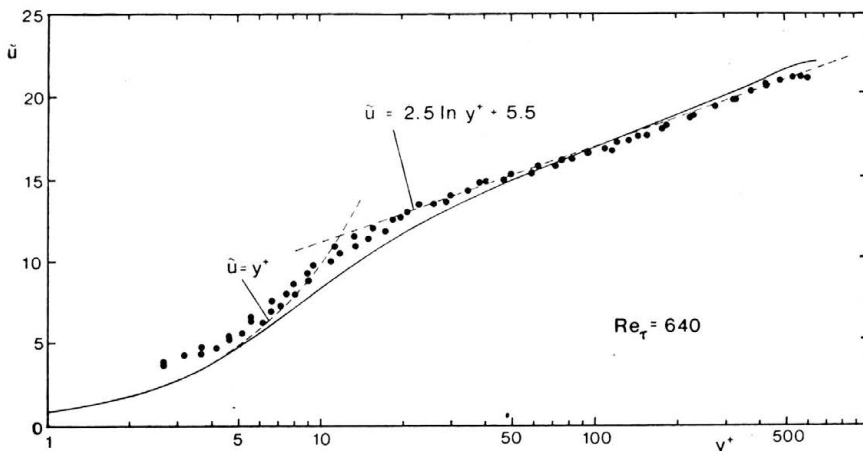


FIG. 7. Mean velocity distribution as calculated by Eq. (5.3) (solid line) compared with experimental data (symbols) of HUSSAIN and REYNOLDS [10].

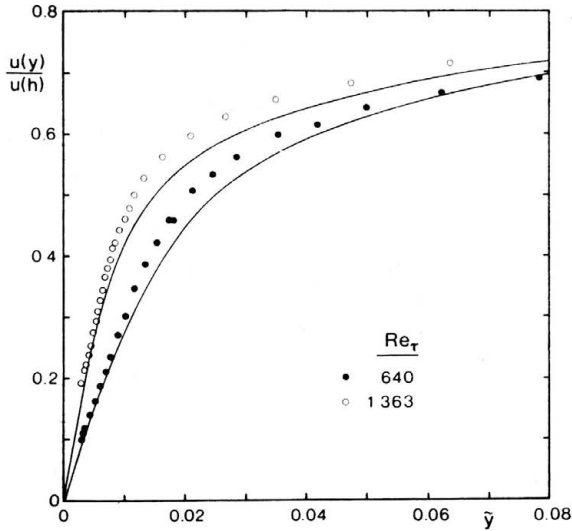


FIG. 8. Mean velocity distribution near the wall as calculated by Eq. (5.3) (solid lines) compared with experimental data of HUSSAIN and REYNOLDS [10].

exhibit the same Reynolds number dependence in the near wall region as the measured mean velocity distributions.

A common feature of all models based on the mixing-length concept is that the resulting eddy viscosity necessarily tends to zero value at the centerline, while experimental evidence, (Fig. 6), indicates that $\varepsilon/u_\tau h$ is about 0.07 as \tilde{y} tends to 1. Previous numerical analyses, however, have indicated that the value of ε near the centerline is not crucial for the solution. For instance, CEBECI and CHANG [4] and CEBECI [3] employed the Cebeci and Chang model, and obtained reasonable results in spite of the vanishing ε at the centerline. However, a consequence of the vanishing eddy viscosity is the drastic reduction of the effective diffusivity in the momentum equation (3.1). According to the heuristic stability analysis of HIRT [8], the restriction imposed on the time step in any explicit numerical solution method depends crucially on the effective viscosity. It is therefore suggested that the influence of the actual model on the numerical stability should be investigated.

6. Conclusions

It has been demonstrated that problems may arise from algebraic eddy viscosity models which explicitly depend on the cross-stream velocity gradient. An alternative formulation which exactly fits to the momentum equation, has been derived by extending van Driest's analysis to fully developed pressure-driven duct flows. The resulting model for the eddy viscosity is implicitly based on a mixing-length formulation, but differs from the usual mixing-length models in that the velocity gradient $\partial u/\partial y$ has been eliminated. Profiles of eddy viscosity and mean velocity obtained by using well-established values for the model constants, compare favourably with experimental results over most of the cross-section. The observed deviation in the ε -distribution near the symmetry line is supposed to be immaterial for the resulting mean velocity profiles.

References

1. H. I. ANDERSSON, *Thin-shear-layer models for two-dimensional free-surface flows in sloping channels*, Dr. ing. Thesis, Norwegian Institute of Technology, Trondheim, 1982.
2. H. I. ANDERSSON and T. YTREHUS, *Thin-shear-layer model in super critical hydraulic flow*, Transactions of the ASME, J. Appl. Mech., **51**, 2, 232–238, 1984.
3. T. CEBECI, *Calculation of momentum and heat transfer in internal flows and in flows with small regions of separation*, in: *Turbulent Forced Convection in Channels and Bundles*, **1**, eds. S. KAKAC and D. B. SPALDING, McGraw-Hill-Hemisphere, Washington, 75–114, 1979.
4. T. CEBECI and K. C. CHANG, *A general method for calculating momentum and heat transfer in laminar and turbulent duct flows*, Num. Heat Transfer, **1**, 1, 39–68, 1978.
5. T. CEBECI and A. M. O. SMITH, *A finite-difference method for calculating compressible laminar and turbulent boundary layers*, Transactions of the ASME, J. Basic Engng., **92**, 3, 523–535, 1970.
6. R. D. CESS, *A survey of the literature in heat transfer in turbulent tube flow*, Westinghouse Research Report 8-0529-R-24, 1958.
7. T. HANSON, D. M. SOMMERS and C. B. WILSON, *Numerical modelling of wind flow over buildings in two dimensions*, Int. J. Num. Met. Fluids, **4**, 1, 25–41, 1984.
8. C. W. HIRT, *Heuristic stability theory for finite-difference equations*, J. Comp. Phys., **2**, 339–355, 1968.
9. C. W. HIRT, *Numerical methods for bluff body aerodynamics*, von Kármán Institute Lecture Series 1984–8 on: *Flow Around Bluff Bodies*, Rhode-St-Genève, 1984.
10. A.K.M.F. HUSSAIN and W.C. REYNOLDS *Measurements in fully developed turbulent channels flow*, Transactions of the ASME, J. Fluids Engng., **97**, 568–578, 1975.
11. J. NIKURADSE, *Gesetzmässigkeit der turbulenten Strömung in glatten Rohren*, VDI-Forschungsheft 356, 1932.
12. S. I. PAI, *On turbulent flow between parallel plates*, Transactions of the ASME, J. Appl. Mech., **20**, 1, 109–114, 1953.
13. L. PRANDTL, *Bericht über Untersuchungen zur ausgebildete Turbulenz*, Z. Angew. Math. Mech., **5**, 136–139, 1925.
14. H. REICHARDT, *Vollständige Darstellung der turbulenten Geschwindigkeitsverteilung in glatten Leitungen*, Z. Angew. Math. Mech., **31**, 7, 208–219, 1951.
15. C. TAYLOR, J. J. HARPER, T. G. HUGHES and K. MORGAN, *An analysis of developing turbulent flow in a circular pipe by the finite element method*, in: *Numerical Methods in Laminar and Turbulent Flow*, eds. C. TAYLOR, K. MORGAN and C. A. BREBBIA, Pentech Press, London, 341–350, 1978.
16. C. TAYLOR, T. G. HUGHES and K. MORGAN, *A numerical analysis of turbulent flow in pipes*, Comp. Fluids, **5**, 4, 191–204, 1977.
17. E. R. VAN DRIEST, *On turbulent flow near a wall*, J. Aero. Sci., **23**, 1007–1011 (1036), 1956.

THE NORWEGIAN INSTITUTE OF TECHNOLOGY, TRONDHEIM, NORWAY.

Received October 25, 1985.